ACS APPLIED ELECTRONIC MATERIALS

pubs.acs.org/acsaelm Letter

Selective Crystallization of Ferroelectric $Hf_xZr_{1-x}O_2$ via Excimer Laser Annealing

Myeong Seop Song, Kunwoo Park, Kyoungjun Lee, Jung Woo Cho, Tae Yoon Lee, Jungwon Park, and Seung Chul Chae*

Cite This: https://doi.org/10.1021/acsaelm.2c01555 Read Online

ACCESS | Metrics & More | Article Recommendations | Supporting Information

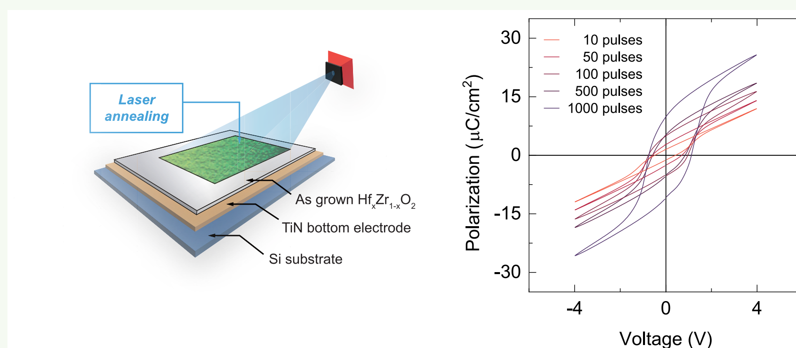

ABSTRACT: Herein, we report the ferroelectricity of $Hf_xZr_{1-x}O_2$ (HZO) thin films crystallized via excimer laser annealing at 25 °C under atmospheric conditions. We characterized the structure and antiferroelectric/ferroelectric properties of HZO thin films using X-ray diffraction and standard polarization−voltage hysteresis. The laser-annealed $Hf_{0.5}Zr_{0.5}O_2$ thin film was gradually crystallized with increasing laser pulse number. The HZO thin film series exhibited systemic changes in antiferroelectric/ferroelectric properties with variations in Zr concentration. In addition, we constructed a phase diagram of laser-annealed HZO thin films.

KEYWORDS: *excimer laser annealing, ferroelectricity, antiferroelectricity, hafnium oxide, zirconium oxide, crystallization*

Downloaded via SEOUL NATL UNIV on January 10, 2023 at 00:45:06 (UTC).
See https://pubs.acs.org/sharingguidelines for options on how to legitimately share published articles.

Extensive fundamental research has been conducted on HfO_2-based ferroelectric thin films since the discovery of ferroelectricity in HfO_2.[1] The unprecedented ferroelectricity with large remnant polarization and coercivity renders the ferroelectric HfO_2 film applicable for next-generation electronic devices, such as ferroelectric field effect transistors (Fe-FETs),[2] synaptic devices,[3] and negative-capacitance field effect transistors (NC-FETs).[4] In contrast to typical ferroelectric perovskites such as $BaTiO_3$ and $Pb(Zr,Ti)O_3$, HfO_2-based ferroelectric thin films exhibit robust ferroelectricity with a few layers and excellent compatibility with Si-based complementary metal−oxide−semiconductor (CMOS) devices.[2] Moreover, the subnanometer-scale localization of electric dipoles and individual switching of the ferroelectric dipoles offer opportunities for ultradense oxide electronics.[5] Owing to such advantages, ferroelectric HfO_2 is a promising candidate for industrial nonvolatile electronic devices.[6]

Extensive research has been devoted to elucidating the origin of ferroelectricity and stabilizing the ferroelectric phase adequate for applications.[7] Ferroelectricity in HfO_2 originates from the noncentrosymmetric orthorhombic $Pca2_1$ phase.[1] To stabilize the orthorhombic phase, stress and strain engineering is generally employed using a dopant and/or a top capping electrode along with a rapid thermal annealing process.[8] However, a high-temperature process is required to crystallize the metastable orthorhombic phase, hindering the rapid development of industrial applications.[9] Thus, several studies have reported new strategies for improving ferroelectric properties at low temperatures. The plasma-enhanced atomic layered deposition (PE-ALD) process achieves high ferroelectricity at a low temperature but is limited to 400 °C.[10] Additionally, the deep ultraviolet (DUV)-assisted annealing method lowers the crystallization temperature to 350 °C.[11] In particular, recently reported crystallization studies using nano-/millisecond laser annealing systems offer new opportunities for back-end-of-line compatible fabrication processes for HfO_2-based ferroelectric devices.[12−14]

The laser annealing method is a mature field of research in crystallizing amorphous silicon and oxide thin films, including SiO_2,[15] TiO_2,[16] and perovskites.[17] The laser annealing process

Received: November 14, 2022
Accepted: January 5, 2023

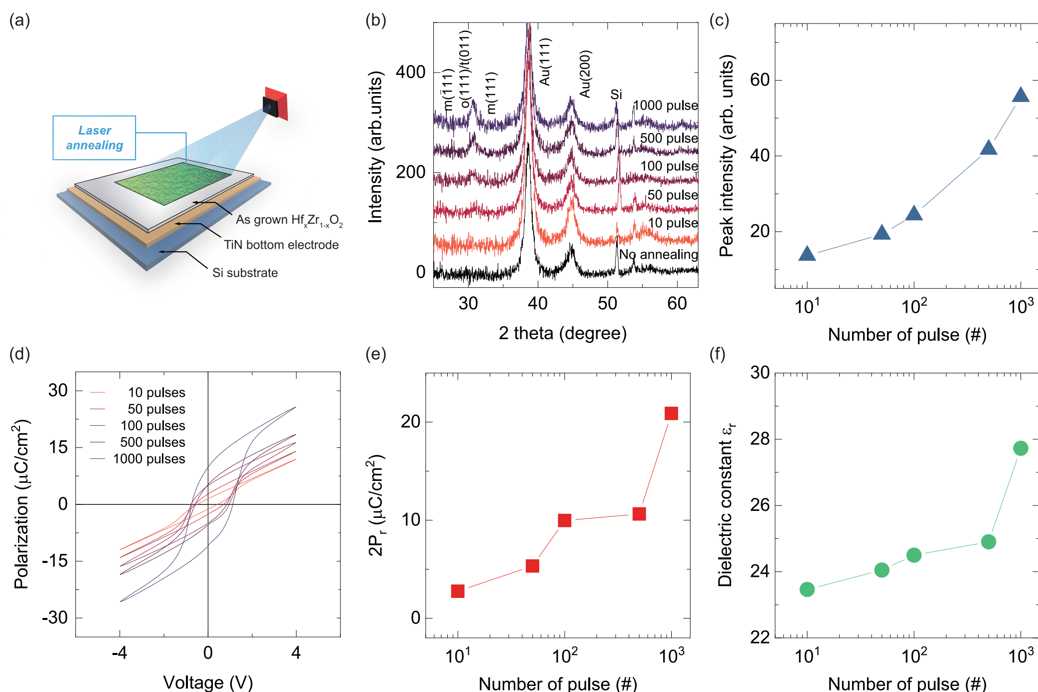

Figure 1. (a) Schematic of HZO/TiN/Si-substrate stack structure annealed by the excimer laser. (b) Grazing incidence X-ray diffraction profiles for the samples annealed under varying the number of excimer laser pulses. (c) X-ray diffraction peak intensity corresponding to cubic-like phases including the tetragonal and orthorhombic phases as a function of the number of laser pulses. (d) Polarization−voltage (P−V) curves with varying the number of laser pulses. (e) $2P_r$ and (f) dielectric constants as a function of the number of laser pulses.

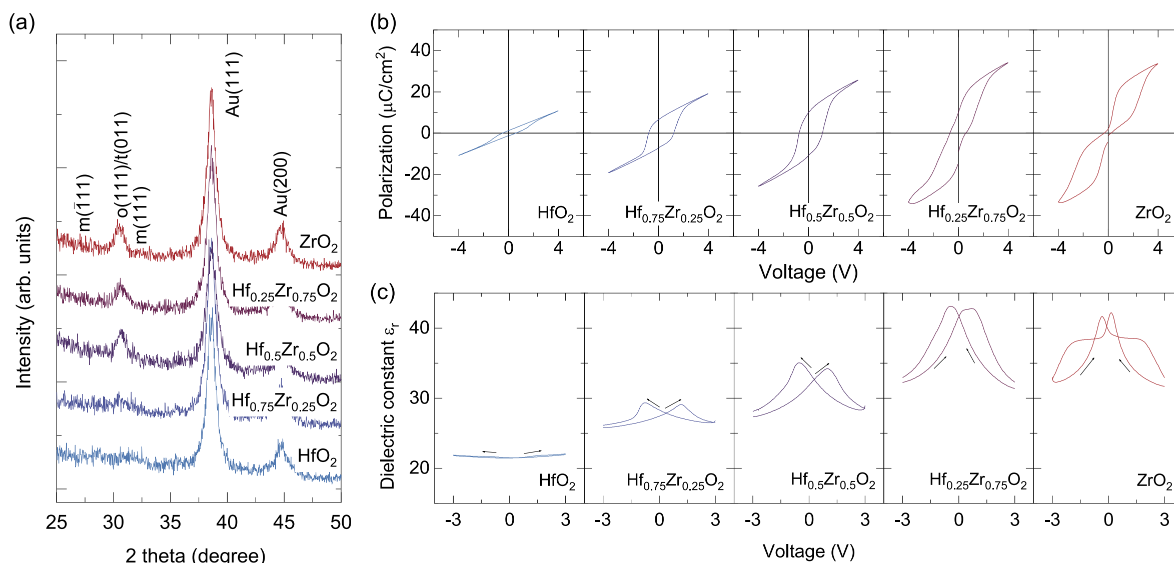

Figure 2. (a) Grazing incidence X-ray diffraction profiles, (b) polarization−voltage, and (c) dielectric constant−voltage hysteresis of 10 nm thick $Hf_xZr_{1-x}O_2$ thin film series. The polarization−voltage and dielectric constant−voltage hysteresis were measured for Au/TiN/$Hf_xZr_{1-x}O_2$/TiN capacitor with an area of 90 × 90 μm^2 and a thickness of 10 nm. The voltage range of the polarization−voltage and dielectric constant−voltage hysteresis is ±4 and ±3 V, respectively.

has the ability to regulate rapid heating and cooling processes by controlling the laser pulse. In addition, a separate photochemical effect allows oriented/epitaxial crystal growth owing to photochemical effect. The nucleation and growth mechanism of the oxide crystal phase using laser annealing depends on the time scale of the radiation input and the absorbance factor of the material. However, few studies have reported an effect of laser annealing in the case of HfO_2.[18] A better understanding of the effect of the laser annealing process in HfO_2 thin films allows for a new degree of freedom with regard to the fabrication of next-generation devices, which are currently difficult to produce via conventional heating processes for stacked device structures.

Herein, we report an experimental investigation of the crystallization of $Hf_xZr_{1-x}O_2$ (HZO) thin film series via the pulsed laser annealing process over a wide range of compositions. With variations in the Zr composition ratio, we observed the systemic changes in antiferroelectric/ferro-

electric properties of laser-annealed HZO thin film. In addition, we reported the selective formation of the orthorhombic phase in $Hf_{0.5}Zr_{0.5}O_2$ thin films via pulsed laser annealing process variations. The results are of technical importance for achieving the ferroelectric properties of the HfO_2-based thin films with a low thermal budget and are helpful for understanding the crystal growth and phase transition through the laser annealing process.

The crystallization of the HZO thin film was enhanced as the number of laser pulses increased. Figure 1b shows the grazing incidence X-ray diffraction (GIXRD) patterns indicating the evolution of $Hf_{0.5}Zr_{0.5}O_2$ crystallinity with varying the number of laser pulses. The pattern of the nonannealed film only has peaks around 38°, 45°, and 53° corresponding to the structure of the gold electrode and silicon substrate. However, the peak around 30.5° corresponding to the cubic-like phase including the orthorhombic phase (111) or tetragonal phase (011) (o(111)/t(011)) gradually rises with increasing pulse irradiation number. Notably, the determination among the tetragonal and orthorhombic phases is certainly ambiguous owing to their similar peak positions in the GIXRD pattern. However, the monoclinic phase exhibits two separated peaks at around 28.5° and 31.6°. Although the growth of the monoclinic phase cannot be completely excluded, it is clear that the crystallization of the cubic-like phase is enhanced by increasing the number of laser pulses. Furthermore, the increase in dielectric constant ε_r and remnant polarization P_r accompanied by the increase in X-ray intensity supports that the laser annealing process selectively enhanced the formation of cubic-like phases in $Hf_{0.5}Zr_{0.5}O_2$ thin films (see Figure 1c,e,f). The $2P_r$, dielectric constant ε_r, and the XRD peak intensity corresponding to the cubic-like phase are plotted as a function of the number of laser pulses. The underlying ε_r−V curves are given in the Supporting Information. Meanwhile, an adequate number of laser pulses is required to achieve optimal crystallization. For polycrystalline growth, sufficient photothermal heating is essential to nucleate an initial crystal in amorphous films without preferential nucleation sites. However, after crystal nucleation, crystal growth is enhanced by photothermal heating and a photochemical effect at the reaction interface on the surface.[18]

The laser annealing process at room temperature in the ambient air demonstrated systemic structural changes in various compositions, similar to the conventional postmetallization annealing (PMA) process. Figure 2a presents the GIXRD patterns of the laser-annealed HZO thin film series. In the high ZrO_2 concentration region, the intensity of the o(111)/t(011) peak was enhanced without peak separation or an additional peak emergence. However, although it is difficult to unambiguously determine the structure phase owing to its low diffraction intensity in the Hf-rich region, the GIXRD pattern exhibits the peaks corresponding to the orthorhombic/tetragonal and monoclinic phases. In the 16 nm thick laser-annealed Hf-rich HZO samples, the o(111)/t(011), monoclinic $(11\bar{1})$, and monoclinic (111) peaks were clearly seen (Figure S3). The enhancement of the orthorhombic/tetragonal phase with increasing Zr concentration was observed as reported by the thermal annealing process.[19] The previously reported thermodynamic model and experimental results demonstrated that the Zr dopant lowers the crystallization temperature and stabilizes the t-/o-phase formation of HZO thin films.[20]

The origin of laser annealing-induced crystallization can be categorized into two mechanisms: photochemical and photothermal effects. Previous research suggested that the pulsed laser process induces the initial crystal nucleation and subsequent advance of crystal growth by the photochemical effect and instantaneous temperature increase by the photothermal effect.[12−14,18] Although crystallized HfO_2 has a large bandgap of ∼5.6 eV, the photothermal heating effect could occur owing to the photoabsorbance of the amorphous layer, bottom electrode, and substrate. The photothermal effect yields a much higher heating and cooling rate than the conventional rapid thermal annealing process. An extremely fast heating process prohibits the growth of the monoclinic phase, considering the thermodynamic stability at a small crystal growth scale.[21] In addition, a fast cooling process promotes the transition of HfO_2 crystalline from the tetragonal to orthorhombic phases by preventing phase relaxation with large tensile stress.[22] Conversely, the photochemical cleavage of organic residues and subsequent scavenging could cause the formation of a dense metal−oxygen−metal bond,[23] causing the facilitated crystallization of HZO thin films. In addition, the photocharged electrons transferred from the bottom TiN electrode to the HZO interfaces can further enhance the crystallization of the HZO thin film.[11]

Because ferroelectricity is intimately related to the crystal structure, ferroelectric characteristics can reveal the distinct differences corresponding to the crystalline structure. The ferroelectricity of HZO thin films originates from the noncentrosymmetric orthorhombic phase.[1] Antiferroelectricity is assumed to originate from the centrosymmetric tetragonal $P4_2/nmc$ and orthorhombic ZrO_2 phases, corresponding to nonpolar and polar phases, respectively.[24,25] Thus, the ferroelectric and antiferroelectric behaviors represent the orthorhombic and tetragonal phase formation in the laser-annealed HZO thin film series, respectively.

Laser-annealed HZO thin films exhibit ferroelectricity over a wide composition range of the solid solution. Figure 2b shows the polarization−voltage (P−V) hysteresis curves for laser-annealed HZO thin films with varying zirconium concentrations. Pure HfO_2 thin film exhibits paraelectric property with small remnant polarization. Almost linear dielectric properties responded to the applied electric field in the pure HfO_2 region. As expected from the analysis of the GIXRD data, introducing Zr in HfO_2 gradually causes the attainment of the ferroelectric property. Maximum remnant polarization was achieved for the $Hf_{0.5}Zr_{0.5}O_2$ film. Increasing the ZrO_2 content in the solid solution reduces the remnant polarization at zero bias, phenomenologically described as superimposed antiferroelectric characteristics.

The high dielectric constant demonstrates dominant orthorhombic/tetragonal phase formation in the laser-annealed HZO thin film series. Figure 2c displays the dielectric constant−voltage curves for laser-annealed HZO thin films with varying Zr concentrations. The peaks in the butterfly-like hysteresis of the dielectric constant−voltage curves result from ferroelectric polarization switching. The dielectric constant outside the peak of the butterfly shape represents the static dielectric contribution. The dielectric constants of the monoclinic, orthorhombic, and tetragonal phases are theoretically known to be 19−25, 24−29, and 24−57, respectively.[26] The increase in the dielectric constant implies that the paraelectric monoclinic phase was relatively suppressed, and the orthorhombic/tetragonal phases were enhanced with

https://doi.org/10.1021/acsaelm.2c01555
ACS Appl. Electron. Mater. XXXX, XXX, XXX−XXX

increasing Zr concentrations. Considering the GIXRD and electrical measurement results, the laser annealing process drives the high-k phase formation and considerably stabilizes the ferroelectric orthorhombic phase in the $Hf_{0.5}Zr_{0.5}O_2$ composition.

The laser annealing process results in the dominant formation of the orthorhombic phase with the large remnant polarization detached from other combined stacking processes such as the top electrode capping. Figure 3a shows a cross-sectional transmission electron microscope (TEM) image of the laser-annealed TiN/10 nm $Hf_{0.5}Zr_{0.5}O_2$/TiN structure. The fast Fourier transform (FFT) image corresponding to the boxed area in Figure 3a is shown in Figure 3b. As evidenced by FFT, the crystal structure was identified as the orthorhombic phase. Considering the results from GIXRD and TEM analysis, the laser annealing process yields the preferential formation of an orthorhombic phase in the $Hf_{0.5}Zr_{0.5}O_2$ thin film. In addition, the largest remnant polarization and square-like hysteresis of $Hf_{0.5}Zr_{0.5}O_2$ thin films support that the laser annealing process induced the dominant formation of the ferroelectric phase among the cubic phases.

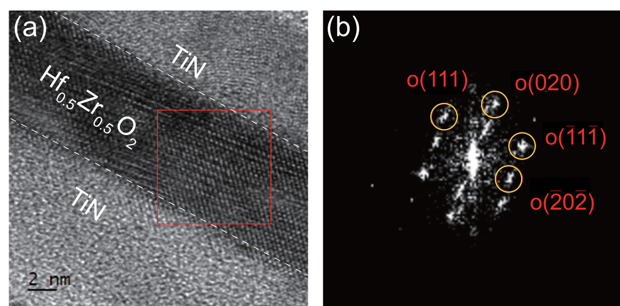

Figure 3. (a) Cross-sectional TEM image of laser-annealed 10 nm $Hf_{0.5}Zr_{0.5}O_2$ film. (b) FFT of partial region (red box) in (a) with orthorhombic spots circled.

The crystallization of metastable orthorhombic phases without a top electrode offers intriguing possibilities for potential advantages of the laser annealing process. Generally, the monoclinic phase is thermodynamically more stable below 1750 °C than the tetragonal and orthorhombic phases.[27] Thus, the nucleated high symmetric phase is likely to transform into the monoclinic phase in conventional thermal annealing processes. A mechanical strain is usually used to stabilize the ferroelectric orthorhombic phase. A TiN capping layer impedes the volume expansion of the transformation from the t- to m-phase during crystallization.[1] Moreover, the potential scavenging effect of the TiN electrode, varying the oxygen vacancy distribution, is attributed to the stabilization of the o-phase.[28] However, the conventional PMA process is feasible in device applications, considering the high thermal budget for the device fabrication process. When HZO films are crystallized without a capping layer via a laser annealing process, the dominant formation of the orthorhombic or tetragonal phase is achieved. Hence, it might be expected that the laser annealing process inhibits the monoclinic phase nucleation from the amorphous state, and controlling the annealing condition selectively allows the formation of tetragonal and orthorhombic phases.

On the basis of the GIXRD data analysis, we constructed a phase diagram of laser-annealed HZO thin films for various compositions and thicknesses. The cubic-like phase ratio estimated from the peak intensity relation of the coinciding integrated intensity of diffraction peak corresponding to the cubic-like phase (I_c) including the tetragonal and orthorhombic phases against the monoclinic (111) and monoclinic (11$\bar{1}$) phases ($I_{m(111)}$ and $I_{m(11\bar{1})}$) is as follows (Figure 4a):[29]

$$\text{cubic-like phase ratio (\%)} = \frac{I_c}{I_{m(111)} + I_{m(11\bar{1})} + I_c}$$

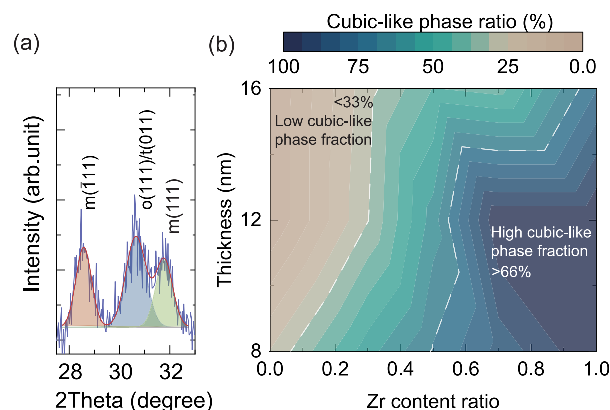

Figure 4. (a) GIXRD peak deconvolution with m(11$\bar{1}$), o(111)/t(011), and m(111) at 28.5°, ≈30.5°, and 31.6°, respectively. (b) Phase diagram for the laser-annealed HZO thin films with varying thickness and composition ratio.

This empirical equation called the "polymorph method" does not take into account all theoretical parameters. However, the estimated result agrees well with the theoretical equation for the analysis of the monoclinic-cubic-like phase ZrO_2 and HfO_2 system.[19,30] For the comparison in terms of structure factor $F(hkl)$, the multiplicity of reflection hkl, and the unit cell volume, see the Supporting Information, Section 6.

Figure 4b shows the variations in the estimated cubic-like phase ratios of the laser-annealed HZO thin films with different compositions and thicknesses. The structural behavior varies from monoclinic to cubic-like phases with increasing Zr concentration ratio and decreasing thickness. The high cubic-like phase ratio and the low cubic-like phase ratio regions are expected to coincide with the emergence of antiferroelectric/ferroelectric-like and paraelectric behaviors, respectively. Even though the phase diagram is limited to the application of the laser annealing process, it is expected to provide a valuable guideline for the crystallization of HZO thin films.

In summary, the crystallization of the HZO thin-film series was demonstrated using a KrF PLA process. Accumulative crystallization was observed on increasing the number of laser pulses. Similar to typical HfO_2−ZrO_2 systems, laser-annealed HZO thin films exhibit dielectric, ferroelectric, and antiferroelectric properties over a wide composition range. Furthermore, a phase diagram of laser-annealed HZO thin films for various compositions and thicknesses was demonstrated. This work could be the key to unraveling the effect of the laser annealing process on the crystallization of HZO thin films. In addition, it provides an opportunity to develop an HZO-based ferroelectric device application through a low thermal-budget process.

https://doi.org/10.1021/acsaelm.2c01555
ACS Appl. Electron. Mater. XXXX, XXX, XXX−XXX

ASSOCIATED CONTENT

Supporting Information

The Supporting Information is available free of charge at https://pubs.acs.org/doi/10.1021/acsaelm.2c01555.

Specific method to fabricate ferroelectric $Hf_xZr_{1-x}O_2$ thin film via pulsed laser annealing process; electrical properties of $Hf_{0.5}Zr_{0.5}O_2$ thin film crystallized by pulsed laser annealing process; grazing incidence X-ray diffraction of 16 nm thick pure HfO_2 and $Hf_{0.75}Zr_{0.25}O_2$ film; scanning electron microscopy of the $Hf_{0.5}Zr_{0.5}O_2$ film; a comparison of the effect between the laser annealing process and the other conventional annealing method; characterization of crystal phases based on the polymorph method (PDF)

AUTHOR INFORMATION

Corresponding Author

Seung Chul Chae − *Department of Physics Education, Seoul National University, Seoul 08826, Republic of Korea;* orcid.org/0000-0002-0913-027X; Email: scchae@snu.ac.kr

Authors

Myeong Seop Song − *Department of Physics Education, Seoul National University, Seoul 08826, Republic of Korea;* orcid.org/0000-0002-9750-8091

Kunwoo Park − *School of Chemical and Biological Engineering, Institute of Chemical Process, Seoul National University, Seoul 08826, Korea*

Kyoungjun Lee − *Department of Physics Education, Seoul National University, Seoul 08826, Republic of Korea;* orcid.org/0000-0003-0472-3583

Jung Woo Cho − *Department of Physics Education, Seoul National University, Seoul 08826, Republic of Korea*

Tae Yoon Lee − *Department of Physics Education, Seoul National University, Seoul 08826, Republic of Korea;* orcid.org/0000-0003-1754-8657

Jungwon Park − *School of Chemical and Biological Engineering, Institute of Chemical Process, Seoul National University, Seoul 08826, Korea; Center for Nanoparticle Research, Institute for Basic Science (IBS), Seoul 08826, Korea;* orcid.org/0000-0003-2927-4331

Complete contact information is available at: https://pubs.acs.org/10.1021/acsaelm.2c01555

Notes

The authors declare no competing financial interest.

ACKNOWLEDGMENTS

This study was supported by the Ministry of Trade, Industry, and Energy of Korea (Grant 10080657), the Korea Semiconductor Research Consortium program for the development of future semiconductor devices, the National Research Foundation of Korea (NRF) grant funded by the Korean government (MSIT) (Grants NRF-2020M3F3A2A01081594 and NRF-2021R1A2C1094795), the Institutes for Basic Science (IBS-R006-D1) (J.P.), and the National Research Foundation of Korea (NRF) grant funded by the Korean government (NRF-2017R1A5A1015365) (J.P.). Part of this study was performed using the facilities of the IBS Center for Correlated Electron Systems, Seoul National University.

REFERENCES

(1) Böscke, T. S.; Müller, J.; Bräuhaus, D.; Schröder, U.; Böttger, U. Ferroelectricity in hafnium oxide thin films. *Appl. Phys. Lett.* **2011**, *99* (10), 102903.

(2) Böscke, T. S.; Müller, J.; Bräuhaus, D.; Schröder, U.; Böttger, U.Ferroelectricity in hafnium oxide: CMOS compatible ferroelectric field effect transistors. In *2011 International Electron Devices Meeting*, 5−7 Dec 2011, 2011; pp 24.25.21−24.25.24.

(3) Mulaosmanovic, H.; Ocker, J.; Müller, S.; Noack, M.; Müller, J.; Polakowski, P.; Mikolajick, T.; Slesazeck, S.Novel ferroelectric FET based synapse for neuromorphic systems. In *2017 Symposium on VLSI Technology*, 5−8 June 2017, 2017; pp T176−T177.

(4) Yu-Chien, C.; Chun-Hu, C.; Chun-Yen, C.; Ying-Tsan, T.; Min-Cheng, C.One-transistor ferroelectric versatile memory: Strained-gate engineering for realizing energy-efficient switching and fast negative-capacitance operation. In *2016 IEEE Symposium on VLSI Technology*, 14−16 June 2016, 2016; pp 1−2.

(5) Lee, H.-J.; Lee, M.; Lee, K.; Jo, J.; Yang, H.; Kim, Y.; Chae, S. C.; Waghmare, U.; Lee, J. H. Scale-free ferroelectricity induced by flat phonon bands in HfO_2. *Science* **2020**, *369* (6509), 1343−1347.

(6) Zhou, Z.; Zhou, J.; Wang, X.; Wang, H.; Sun, C.; Han, K.; Kang, Y.; Zheng, Z.; Ni, H.; Gong, X. A Metal-Insulator-Semiconductor Non-Volatile Programmable Capacitor Based on a $HfAlO_x$ Ferroelectric Film. *IEEE Electron Device Lett.* **2020**, *41* (12), 1837−1840.

(7) Park, M. H.; Lee, Y. H.; Kim, H. J.; Kim, Y. J.; Moon, T.; Kim, K. D.; Müller, J.; Kersch, A.; Schroeder, U.; Mikolajick, T.; Hwang, C. S. Ferroelectricity and Antiferroelectricity of Doped Thin HfO_2-Based Films. *Adv. Mater.* **2015**, *27* (11), 1811−1831.

(8) Xu, L.; Nishimura, T.; Shibayama, S.; Yajima, T.; Migita, S.; Toriumi, A. Kinetic pathway of the ferroelectric phase formation in doped HfO_2 films. *J. Appl. Phys.* **2017**, *122* (12), 124104.

(9) Park, M. H.; Kim, H. J.; Kim, Y. J.; Lee, W.; Moon, T.; Hwang, C. S. Evolution of phases and ferroelectric properties of thin $Hf_{0.5}Zr_{0.5}O_2$ films according to the thickness and annealing temperature. *Appl. Phys. Lett.* **2013**, *102* (24), 242905.

(10) Onaya, T.; Nabatame, T.; Sawamoto, N.; Ohi, A.; Ikeda, N.; Nagata, T.; Ogura, A. Ferroelectricity of $Hf_xZr_{1-x}O_2$ thin films fabricated by 300 °C low temperature process with plasma-enhanced atomic layer deposition. *Microelectron. Eng.* **2019**, *215*, No. 111013.

(11) Joh, H.; Anoop, G.; Lee, W.-J.; Das, D.; Lee, J. Y.; Kim, T. Y.; Kim, H.; Seol, W.; Yeom, J.; Jeon, S.; Hong, S.; Yoon, M.-H.; Jo, J. Y. Low-Temperature Growth of Ferroelectric $Hf_{0.5}Zr_{0.5}O_2$ Thin Films Assisted by Deep Ultraviolet Light Irradiation. *ACS Applied Electronic Materials* **2021**, *3* (3), 1244−1251.

(12) Tabata, T. Nucleation and crystal growth in HfO_2 thin films by UV nanosecond pulsed laser annealing. *Applied Physics Express* **2020**, *13* (1), No. 015509.

(13) Tabata, T.; Halty, S.; Rozé, F.; Huet, K.; Mazzamuto, F. Non-doped HfO_2 crystallization controlled by dwell time in laser annealing. *Applied Physics Express* **2021**, *14* (11), 115503.

(14) Volodina, N.; Dmitriyeva, A.; Chouprik, A.; Gatskevich, E.; Zenkevich, A. Ferroelectric $Hf_{0.5}Zr_{0.5}O_2$ Thin Films Crystallized by Pulsed Laser Annealing. *physica status solidi (RRL) − Rapid Research Letters* **2021**, *15* (5), No. 2100082.

(15) Kitsomboonloha, R.; Baruah, S.; Myint, M. T. Z.; Subramanian, V.; Dutta, J. Selective growth of zinc oxide nanorods on inkjet printed seed patterns. *J. Cryst. Growth* **2009**, *311* (8), 2352−2358.

(16) Tsuchiya, T.; Watanabe, A.; Imai, Y.; Niino, H.; Yamaguchi, I.; Manabe, T.; Kumagai, T.; Mizuta, S. Direct Conversion of Titanium Alkoxide into Crystallized TiO_2 (rutile) Using Coating Photolysis Process with ArF Excimer Laser. *Jpn. J. Appl. Phys.* **1999**, *38* (7B), L823−L825.

(17) Nakajima, T.; Tsuchiya, T.; Ichihara, M.; Nagai, H.; Kumagai, T. Epitaxial Growth Mechanism for Perovskite Oxide Thin Films under Pulsed Laser Irradiation in Chemical Solution Deposition Process. *Chem. Mater.* **2008**, *20* (23), 7344−7351.

(18) Nakajima, T.; Shinoda, K.; Tsuchiya, T. UV-assisted nucleation and growth of oxide films from chemical solutions. *Chem. Soc. Rev.* **2014**, *43* (7), 2027−2041.

(19) Müller, J.; Böscke, T. S.; Schröder, U.; Mueller, S.; Bräuhaus, D.; Böttger, U.; Frey, L.; Mikolajick, T. Ferroelectricity in Simple Binary ZrO_2 and HfO_2. *Nano Lett.* **2012**, *12* (8), 4318−4323.

(20) Park, M. H.; Lee, Y. H.; Kim, H. J.; Schenk, T.; Lee, W.; Kim, K. D.; Fengler, F. P. G.; Mikolajick, T.; Schroeder, U.; Hwang, C. S. Surface and grain boundary energy as the key enabler of ferroelectricity in nanoscale hafnia-zirconia: a comparison of model and experiment. *Nanoscale* **2017**, *9* (28), 9973−9986.

(21) Navrotsky, A. Thermochemical insights into refractory ceramic materials based on oxides with large tetravalent cations. *J. Mater. Chem.* **2005**, *15* (19), 1883−1890.

(22) Ku, B.; Choi, S.; Song, Y.; Choi, C.Fast Thermal Quenching on the Ferroelectric Al:HfO_2 Thin Film with Record Polarization Density and Flash Memory Application. In *2020 IEEE Symposium on VLSI Technology*, 16−19 June 2020, 2020; pp 1−2.

(23) Sundaram, S. K.; Mazur, E. Inducing and probing non-thermal transitions in semiconductors using femtosecond laser pulses. *Nat. Mater.* **2002**, *1* (4), 217−224.

(24) Böscke, T. S.; Teichert, S.; Bräuhaus, D.; Müller, J.; Schröder, U.; Böttger, U.; Mikolajick, T. Phase transitions in ferroelectric silicon doped hafnium oxide. *Appl. Phys. Lett.* **2011**, *99* (11), 112904.

(25) Park, M. H.; Hwang, C. S. Fluorite-structure antiferroelectrics. *Rep. Prog. Phys.* **2019**, *82* (12), 124502.

(26) Materlik, R.; Künneth, C.; Kersch, A. The origin of ferroelectricity in $Hf_{1-x}Zr_xO_2$: A computational investigation and a surface energy model. *J. Appl. Phys.* **2015**, *117* (13), 134109.

(27) STACY, D. W.; WILDER, D. R. The Yttria-Hafnia System. *J. Am. Ceram. Soc.* **1975**, *58* (7−8), 285−288.

(28) Lomenzo, P. D.; Zhao, P.; Takmeel, Q.; Moghaddam, S.; Nishida, T.; Nelson, M.; Fancher, C. M.; Grimley, E. D.; Sang, X.; LeBeau, J. M.; Jones, J. L. Ferroelectric phenomena in Si-doped HfO_2 thin films with TiN and Ir electrodes. *J. Vac. Sci. Technol. B* **2014**, *32* (3), No. 03D123.

(29) Garvie, R. C.; Nicholson, P. S. Phase Analysis in Zirconia Systems. *J. Am. Ceram. Soc.* **1972**, *55* (6), 303−305.

(30) Toraya, H.; Yoshimura, M.; Sōmiya, S. Quantitative Analysis of Monoclinic-Stabilized Cubic ZrO2 Systems by X-Ray Diffraction. *J. Am. Ceram. Soc.* **1984**, *67* (9), C-183−C-184.